SCALE INFLUENCE ON THE ENERGY DEPENDENCE OF PHOTON-PROTON CROSS SECTIONS AND F_2 AT LOW Q^2

N.Z. GOGITIDZE

DESY, Notkestr. 85, D-22603 Hamburg, Germany
and LPI RAS, 117924 Moscow, Russia

New results of a measurement of the proton structure function $F_2(x, Q^2)$ and the total virtual photon-proton cross section are presented for momentum transfer squared Q^2 between 0.35 GeV^2 and 3.5 GeV^2 and for Bjorken-x values down to $6 \cdot 10^{-6}$ using data collected by the HERA experiment H1. The results are compared to phenomenological models at low Q^2. The slope of the W dependence of the cross sections is studied as function of the scale Q^2. In a second study, the scale dependence of the evolution of photoproduction cross sections with the photon-proton centre of mass energy W is studied using low $Q^2 < 0.01$ GeV^2 e^+p interactions. The charged particle with the largest transverse momentum in the photon fragmentation region is used to define the hard scale of the interactions. The slope of the W dependence of the cross section is observed to increase steeply with increasing transverse momentum. The result is compared to measurements of the Q^2 evolution of the W dependence of the virtual photon-proton cross section, as obtained in the first study presented here. Interpretations in terms of QCD and in terms of Regge phenomenology are discussed.

1 Introduction

The energy dependence of the real photon-proton cross section is consistently described at high energies by the power law $\sigma^{tot}_{\gamma p} \propto (W^2)^{\lambda}$, where W is the γp centre of mass energy and the power $\lambda \approx 0.08$ [1,2]. The value $\lambda \approx 0.08$ is found to be universal for all photon or hadron interactions with protons [3]. In contrast, the virtual photon-proton cross section, which at large W is related to the structure function F_2 via $\sigma^{tot}_{\gamma^* p} \approx 4\pi^2\alpha/Q^2 \cdot F_2(W^2, Q^2)$, is found to rise fast with increasing W^2 for Q^2 values larger than a few GeV^2 [4,5]. Here Q^2 is the virtuality of the photon and α the fine structure constant. In the HERA regime fits of the form $\sigma^{tot}_{\gamma^* p} \propto (W^2)^{\lambda}$ lead to values of λ which rise from 0.2 to 0.4 in the Q^2 range from 1.5 to 10^3 GeV^2 [4].

The change of the slope parameter λ with increasing Q^2 is associated with a transition from the non-perturbative 'soft' to the perturbative 'hard' regime [6,7]. Indeed, in the domain where Q^2 is larger than a few GeV^2 and perturbative QCD (pQCD) can be safely applied, it predicts an increase of λ with Q^2. In the domain of 'soft' interaction phenomenology the change of λ can be interpreted in Reggeon Field Theory as a reduction of screening corrections with increasing Q^2 [8]. Reggeon Field Theory and perturbative QCD are two complementary approaches which successfully describe physics processes in different regimes. But the transition region between these soft and hard regimes is not yet well understood.

Here, in order to bring more understanding of this transition region, we select a certain process, define a scale which allows the transition region to be probed and study the energy behaviour of the corresponding cross sections.

Whereas in deep inelastic scattering (DIS) the hardness of the interaction (scale) can be characterized by the momentum transfer squared Q^2, it is the large p_t of the final state hadrons which indicates a hard scattering process in photoproduction ($Q^2 \approx 0$). For the interaction with the proton a high value of Q^2 may indeed play a similar role as production of high p_t particles in the photon fragmentation region.

The results presented in the following have recently been published [9].

2 HERA kinematics and the H1 detector

At the collider HERA 27.5 GeV positrons and 820 GeV protons collide, producing e^+p interactions at a centre of mass energy $\sqrt{s} = 300$ GeV in a wide range of Q^2, from the regime of quasi real photoproduction ($Q^2 \approx 0$) to DIS at large Q^2. The hadronic final state can be detected in the same experiment for both kinds of interactions. Therefore, HERA provides an ideal testing ground to study the transition from soft to hard physics by comparing real and virtual photon-proton collisions.

The H1 detector [10] covers almost 4π of the solid angle and consists, viewed outwards from the interaction point, of tracking detectors, calorimeters and muon detectors. During the winter shutdown 1994/1995 a new calorimeter and a new tracking chamber with increased acceptance for small scattering angles were installed in the backward (electron beam direction) region. In the analyses presented here data come both from the data-taking period with nominal interaction vertex, and from a short period with the interaction vertex shifted downstream by 70 cm. This shift increases the acceptance for electrons scattered through small angles. As a result, the kinematic range in DIS was extended in Q^2 and x down to $Q^2 \sim 0.3$ GeV^2 and $x \sim 6 \cdot 10^{-6}$. x is the Bjorken scaling variable, which is related to W by $W^2 = Q^2/x$.

3 A measurement of the Proton Structure Function $F_2(x, Q^2)$ at low x and Q^2

The measured ep cross section in the HERA kinematic range can be expressed either in terms of proton structure functions or the virtual photon-proton cross section as follows

$$\begin{aligned} \frac{d^2\sigma_{ep}}{dx dQ^2} &= \frac{2\pi\alpha^2}{Q^4 x}(2-2y+\frac{y^2}{1+R})F_2(x,Q^2) \\ &= \Gamma[\sigma_T(x,Q^2)+\epsilon(y)\sigma_L(x,Q^2)] \equiv \Gamma\sigma^{eff}_{\gamma^* p}(x,y,Q^2). \end{aligned} \tag{1}$$

Here σ_L and σ_T are the cross sections for the transverse and longitudinally po-

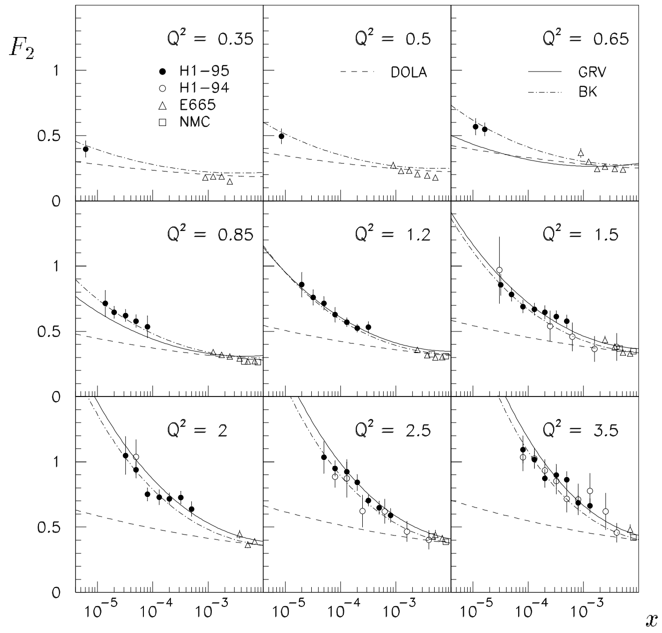

Figure 1: Measurements of the proton structure function $F_2(x,Q^2)$ at low Q^2 from H1 and from fixed target experiments, compared to different model predictions specified in the text.

larized virtual photons, Γ is a flux factor and ϵ is the ratio of the longitudinal to the transverse flux. R is the ratio $F_L/(F_2-F_L)$ where F_L is the longitudinal structure function. To extract the structure function F_2 from these measurements of the ep cross section, an assumption has to be made for the longitudinal structure function F_L since it is not yet measured in this kinematic region. The Badelek - Kwiecinski model [11] is applied for calculating R [a]. This model is based on the photon-gluon fusion process and has the proper

[a] Note that this is an arbitrary choice of R. As long as R is specified together with the extracted F_2, another choice of R can easily be applied for a new derivation of F_2 from the measured σ_{ep}.

limit for $Q^2 \to 0$ where F_L should vanish $\propto Q^4$. In our kinematic range R has values between 0.1 and 0.3, and the effect on the F_2 measurements is rather small. In Fig.1 the F_2 data are shown as function of x in 9 different Q^2 bins. The data are compared with previous H1 measurements [12] and with the fixed target measurements [13,14]. In the overlapping Q^2 bins the new results are in good agreement with the previous measurements. The total error has been reduced by a factor 2 to 3. F_2 is seen to rise steeply with decreasing x for $Q^2 \geq 2$ GeV^2, while for smaller Q^2 values this rise is less steep. The data also show a smooth continuous transition towards the low x region.

The data are compared (see Fig.1) with several model predictions for F_2 at low x. The model of Donnachie and Landshoff (DOLA) [15] assumes a pomeron intercept of $1+\lambda \sim 1.08$ for the energy dependence of the cross section, independent of the virtuality of the photon. The model gives a prediction of F_2 which is too low for $Q^2 \geq 0.85$ GeV^2, but which approaches the data for the lowest Q^2 values. The DOLA prediction can also be interpreted as the contribution of soft pomeron exchange to the cross section at non-zero Q^2. Contrary to this Regge inspired model, the model of Glück, Reya and Vogt

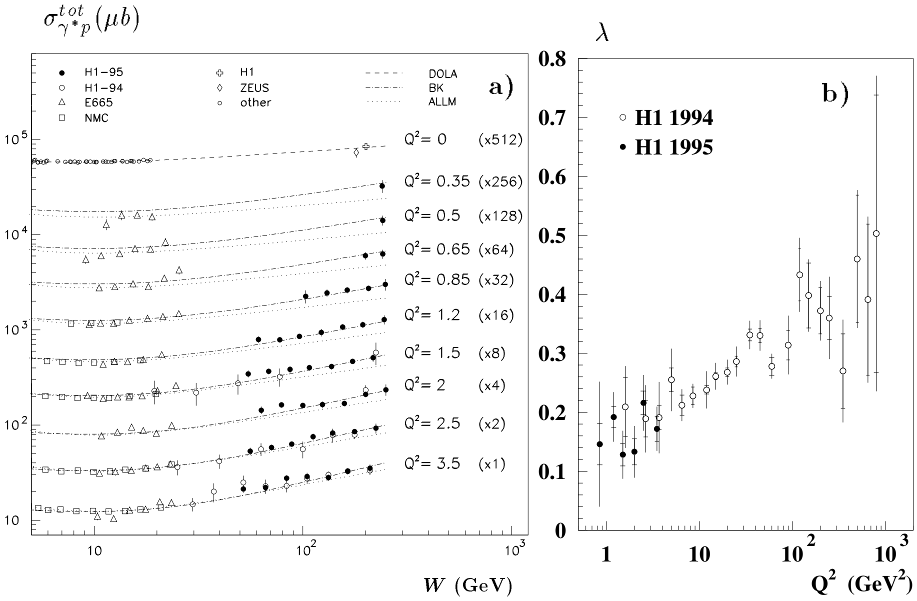

Figure 2: a) The virtual photon-proton cross section $\sigma^{tot}_{\gamma^* p}$ as function of W in different Q^2 bins. The curves represent Donnachie and Landshoff (dashed line), Badelek and Kwiecinski (dashed-dotted line) and Abramowicz et al. (dotted line) parametrizations. b) The slope λ of the W^2 dependence of the proton structure function F_2, as function of Q^2.

(GRV) [16] is defined completely within the parton picture. It is assumed that all parton distributions at very low $Q_0^2 = 0.34$ GeV^2 have a valence-like shape, i.e. vanish for $x \to 0$. Assuming further that F_2 evolves towards large Q^2 values via parton radiation, given by the leading twist QCD evolution equations, GRV predict that the structure function F_2 should rise with decreasing x, even for low values of $Q^2 \sim 1$ GeV^2. The GRV distributions describe the data well for $Q^2 \geq 1$ GeV^2, but fail for $Q^2 < 1$ GeV^2. At low Q^2 values the QCD evolution covers too small a Q^2 range, and the parton distributions become dominated by the valence behaviour at the starting scale Q_0^2. The model of Badelek and Kwiecinski (BK) [17] combines the concepts of Vector Meson Dominance (VMD) with dynamical parton models such as the GRV model. It has per force a smooth transition from pQCD to the real photon limit, which coincides with the region measured here. The BK model predicts F_2 well for all Q^2 bins.

The total virtual photon-proton cross section is here defined as

$$\sigma_{\gamma^* p}^{tot} = \sigma_T(x, Q^2) + \sigma_L(x, Q^2) \simeq \frac{4\pi^2\alpha}{Q^2} F_2(x, Q^2). \tag{2}$$

With this definition $\sigma_{\gamma^* p}^{tot}$ depends only on Q^2 and x (or W) and the results of different experiments may easily be compared. The W dependence of $\sigma_{\gamma^* p}^{tot}$ is shown in Fig.2a in different Q^2 bins. The data are compared with low energy measurements and with photoproduction data. It is observed that $\sigma_{\gamma^* p}^{tot}$ rises faster with increasing W when Q^2 increases. To quantify this observation fits of the F_2 data in the form $F_2 \propto x^{-\lambda}$ ($\sim W^{2\lambda}$) were made in the Q^2 bins. The results of these fits are shown in Fig.2b, where λ is presented as function of Q^2 together with previous H1 measurements. The data confirm the trend already observed in the previous measurements. When $Q^2 \to 0$, data tend towards the 'soft' pomeron limit. The new data show that the transition towards this limit is smooth and continuous. Thus, in this study the intrinsically 'hard' DIS process is used, and the scale Q^2 was followed towards lower values into the transition region.

4 Scale Influence on the Energy Dependence of Photon - Proton Cross Sections

Another way to study the transition region is to use high p_t charged particles as a measure of a typical scale in photoproduction processes, a scale which can be varied in a similar way as the scale Q^2 in DIS.

In total about two million photoproduction events were selected in the scaled energy range $0.25 < y = 1 - E_{e'}/E_e < 0.70$, where E_e and $E_{e'}$ are the initial and scattered positron energies respectively. The corresponding energy range is $150 < W_{\gamma p} < 250$ GeV. The W dependence of the cross section is then measured in different bins of maximum p_t ($p_{t,max}$) of the charged particles.

Good detector acceptance and high resolution of p_t measurements, together with large statistics of photoproduction events, allow a continuous coverage of both soft and hard scattering domains. The acceptance and resolution requirements limit the charged particles to the pseudo-rapidity range $1.1 < \eta^* < 3.1$. η^* = -ln(tan($\theta^*/2$)) is measured with respect to the γ direction in the γp centre of mass system, where θ^* is the polar angle.

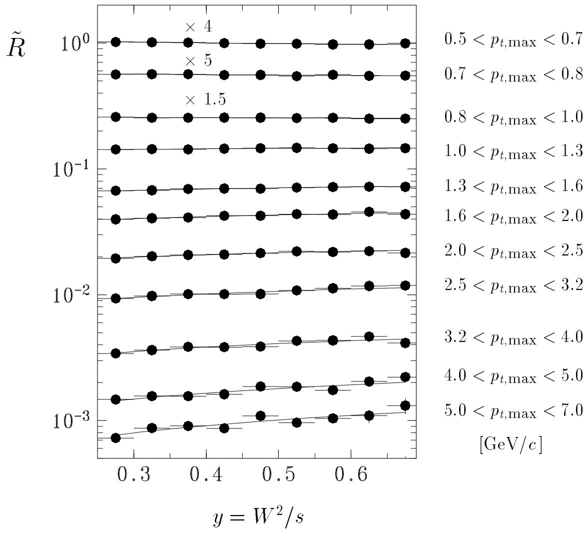

Figure 3: Energy dependence of the ratio $\tilde{R}$ in different bins of $p_{t,max}$. The curves represent fits $\tilde{R} = W^{2 \cdot \tilde{\lambda}}$

In Fig.3 the energy dependence of the ratio of the partial γp cross section to the total γp cross section (which is equal to the ratio $\tilde{R}$ of observed numbers of events) is shown for different $p_{t,max}$ bins. The higher the $p_{t,max}$ values, the steeper is the rise of the ratio with increasing $W_{\gamma p}$.

To quantify this observation fits of the data were made (similar to the ones made in our first study) in the form $\sigma_{\gamma p}(W, p_{t,max}^2) \propto W^{2\lambda(p_{t,max}^2)}$, with the scale defined by the maximum p_t charged particles in the photon fragmentation region. The results of these fits are shown in Fig.4,where the slope λ is given as function of $4p_{t,max}^2$. A strong increase of λ is observed with increasing $p_{t,max}$, as well as a smooth transition from lower to higher values of $p_{t,max}$, so that the data are well fitted by a straight line. Is this rise an effect of phase space

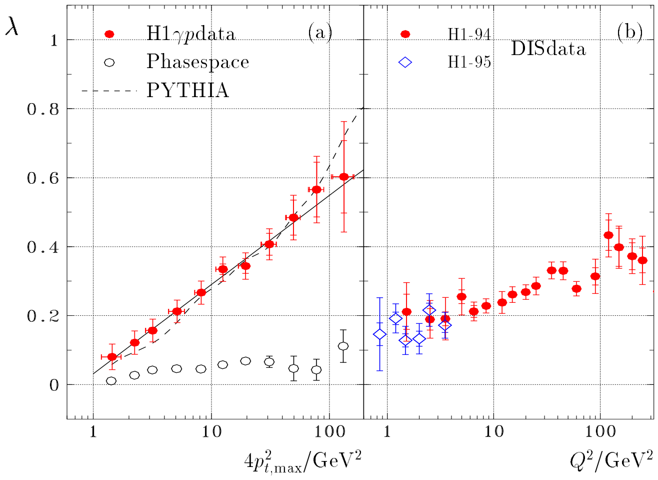

Figure 4: Slope λ of the W^2 dependence dependence of the photoproduction and DIS cross sections as function of $4p_t^2$ and Q^2 respectively.

increase with increasing of $p_{t,max}$? Comparison with a longitudinal phase space model (Fig.4) shows that the phase space effects play only a minor role.

In Fig.4 the date are also compared with the PYTHIA model predictions [18]. The model is based on the Monte Carlo version which includes both pQCD for the hard scattering process and a Regge inspired soft interaction component. Seing that PYTHIA reproduces the trend of the data well it is interesting to understand the reason for this agreement. A study of the different ingredients of the model shows that the main part of the rise can be explained by the integration of the leading order matrix elements over the available phase space. The effects of using different proton and photon structure functions are small. Parton showers, simulating next to leading order effects as well as multiple parton-parton scattering, also give only a small effect. Therefore, the change of the slope λ is not associated with the growth of the gluon density in the proton at small x, contrary to the naive expectation.

5 Conclusions

In summary, a clear similarity is seen in the evolutions of the W dependence of γp and $\gamma^* p$ cross sections with increasing scales ($4p^2_{t,max}$ and Q^2 respectively). Another interesting observation is that the transition from soft to hard regimes is smooth in both cases. This similarity can be qualitatively understood both in terms of pQCD and in terms of a Regge approach. In pQDC the effect of more steeply rising cross sections with increasing hard scale can be readily explained by leading order partonic scattering contributions [19], while in Reggeon Field Theory it is a consequence of the reduction of unitarity corrections to one-pomeron exchange.

Acknowledgments

It is a pleasure for me to thank all my colleagues in H1 for useful discussions and help in preparing the report. I would like to thank the organizers for hospitality and for creating a pleasant and inspiring conference atmosphere.

References

1. H1 Collab., S.Aid et al., *Z. Phys.* C **69**, 27 (1995).
2. ZEUS Collab., M.Derrick et al., *Z. Phys.* C **63**, 391 (1994).
3. A.Donnachie and P.V.Landshoff, *Phys. Lett.* B **296**, 227 (1992); H.Cheng, J.K.Walker and T.T.Wu, *Phys. Lett.* B **44**, 97 (1973).
4. H1 Collab., I.Abt et al., *Nucl. Phys.* B **407**, 515 (1993); H1 Collab., T.Ahmed et al., *Nucl. Phys.* B **439**, 471 (1995); H1 Collab., S.Aid et al., *Nucl. Phys.* B **470**, 3 (1996).
5. ZEUS Collab., M.Derrick et al., *Phys. Lett.* B **316**, 412 (1993); ZEUS Collab., M.Derrick et al., *Z. Phys.* C **65**, 379 (1995); ZEUS Collab., M.Derrick et al., *Z. Phys.* C **69**, 607 (1996).
6. J.Bartels, DIS and QCD, Eds. J.-P.Laporte and Y.Sirois, (1995) 105.
7. A.Levy, TAUP 2349-96 (1996).
8. A.Capella et al., *Phys. Lett.* B **337**, 358 (1994).
9. H1 Collab., S.Aid et al., DESY-97-042 (1997); H1 Collab., S.Aid et al., *Phys. Lett.* B **392**, 234 (1997).
10. H1 Collab., I.Abt et al., *Nucl. Instrum. Methods* A **386**, 310 (1997).
11. B.Badelek, J.Kwiecinski and A.Stasto, Durham DTP /96/16 (1996).
12. H1 Collab., S.Aid et al., *Nucl. Phys.* B **470**, 3 (1996).
13. E665 Collab., M.R.Adams et al., *Phys. Rev.* D **54**, 3006 (1996).
14. NMC Collab., M.Arneodo et al., *Phys. Lett.* B **364**, 107 (1995).
15. A.Donnachie and P.V.Landshoff, *Z. Phys.* C **61**, 139 (1994).
16. M.Glück, E.Reya and A.Vogt, *Z. Phys.* C **67**, 433 (1995).
17. B.Badelek and J.Kwiecinski, *Phys. Lett.* B **295**, 263 (1992).
18. T.Sjöstrand, CERN-TH-6488 (1992).
19. D.Cline, F.Halzen and J.Luthe, *Phys. Rev. Lett.* **31**, 493 (1973); W.Buchmüller and D.Haidt, DESY-96-061 (1996).